

# Polydispersed rods on the square lattice

Jürgen F. Stilck<sup>1,\*</sup> and R. Rajesh<sup>2,†</sup>

<sup>1</sup>*Instituto de Física and National Institute of Science and Technology for Complex Systems,  
Universidade Federal Fluminense, Av. Litorânea s/n, 24210-346 - Niterói, RJ, Brazil*

<sup>2</sup>*The Institute of Mathematical Sciences, C.I.T. Campus, Taramani, Chennai 600113, India*  
(Dated: March 3, 2022)

We study the grand-canonical solution of a system of hard polydispersed rods placed on the square lattice using transfer matrix and finite size scaling calculations. We determine the critical line separating an isotropic from a nematic phase. No second transition to a disordered phase is found at high density, contrary to what is observed in the monodispersed case. The estimates of critical exponents and the central charge on the critical line are consistent with the Ising universality class.

PACS numbers: 05.50+q, 64.60.Cn, 64.70.M-

## I. INTRODUCTION AND DEFINITION OF THE MODEL

The question of the existence of an ordering transition in a system of long rigid rods with only excluded volume interactions is relevant to the study of many physical systems. Examples include liquid crystals [1], tobacco mosaic virus [2] and carbon nanotube gels [3]. In a seminal paper, Onsager showed that, for large enough density and aspect ratio of cylindrical rods, the system undergoes a discontinuous phase transition from an isotropic to an orientationally ordered nematic phase in three dimensions [4]. The case of discrete positions of the rods was considered by Flory [5] and a model of rods in a continuum space but with a discrete set of orientations was studied by Zwanzig [6], with similar results. A review of these continuum models may be found in Ref. [7]. In two dimensions, with continuous positions and orientations of the rods, it is known that the rotational symmetry can not be broken [8], but a Berezinskii-Kosterlitz-Thouless transition [9–11] is found between a low density phase with exponentially decaying orientational correlation and a high density phase where the correlations decay with a power law [12–15].

The lattice version of the problem, where the rods are composed of  $k$  collinear and consecutive sites of a regular lattice ( $k$ -mers), has also been studied in the literature. Here, a lattice site may be occupied by utmost one  $k$ -mer. For the particular case of dimers ( $k = 2$ ), it is known that there is no ordering transition at finite density of unoccupied sites in any dimension [16–19], even though additional interactions can result in an ordering transition [20–22]. For longer rods, Ghosh and Dhar [23] numerically showed the existence of a nematic phase for  $k \geq k_{\min}$  where  $k_{\min} = 7$  on a square lattice, following which the existence of the nematic phase has been proved rigorously for  $k \gg 1$  [24]. However, the fully

packed phase is expected to be disordered [1, 23], resulting in a second transition from nematic to disordered phase at high densities. This has been demonstrated numerically [25, 26]. A solution of the model on a Bethe-like lattice leads to continuous or discontinuous isotropic-nematic transitions for sufficiently high values of  $k$ , depending of the coordination number of the lattice. The second transition does not occur on such a lattice [27], although two transitions are found on a Bethe-like lattice if additional repulsive interactions between the rods are included [28].

Detailed Monte Carlo studies of the first transition show that it is in the Ising universality class on the square lattice and the three state Potts universality class on the triangular and hexagonal lattices, as would be expected from the symmetry of the ordered phase [29–33]. The study of the second transition using simulations is more difficult due to the presence of long-lived metastable states, but these difficulties were overcome using an efficient grand-canonical Monte Carlo algorithm [25, 26]. On the triangular lattice these simulations indicate that the high density transition is also in the three-states Potts universality class, but on the square lattice, due to strong orientational correlations in the high density disordered phase, although non-Ising effective exponents were found, it was not possible to rule out a crossover to Ising exponents at larger system sizes than what were studied. Another generalization of the model is to consider hard rectangles, comprising  $m \times mk$  sites on the square lattice [34–36], and in some cases up to three entropy driven transitions were found with increasing density for  $m > 1$ .

In all the cases discussed above, the rods were monodispersed, but polydispersity in rod lengths may hardly be avoided in experimental situations [37, 38]. From a theoretical point of view its effects on the phase transitions found in the models are interesting [7]. In continuous models, calculations show that polydispersity may have strong effects on the behavior of the system, such as a larger density gap of the discontinuous nematic transition, higher nematic order parameter for the longer rods in the nematic phase, reentrant nematic phase and even two distinct nematic phases coexisting with the isotropic

\* jstilck@if.uff.br

† rrajesh@imsc.res.in

phase [39–42]. Similar results are obtained within the polydispersed Zwanzig model with restricted orientations [43, 44].

Polydispersed systems on lattices are less well studied. One question of interest is whether a second transition to the high density disordered phase, present in monodispersed systems, will persist in a polydispersed system. We recall the argument for the fully packed limit of monodispersed systems being disordered [1, 23]. In its simplest version, it consists of dividing the lattice into  $k \times k$  squares, so that in each square the  $k$  rods may be all either horizontal or vertical. This establishes a lower bound to the entropy per site of the disordered phase  $s \geq k^{-2} \ln 2$ , which is larger than the vanishing entropy of the fully ordered nematic phase. For polydispersed system, the fully nematic phase clearly has non-zero entropy, making it unclear its effect on the high density transition. If the high density phase persists, then it raises the interesting scenario of the fully packed system undergoing a isotropic–nematic transition.

In this paper, we study the phase transitions and critical behavior of a particular model of polydispersed hard rods on the square lattice. The model we consider is inspired by the equilibrium polymerization model that was used, among other applications, to study the polymerization transition of liquid sulfur [45, 46]. The statistical weight of a rod comprising  $k$  successive collinear sites is equal to  $z_i^{k-2} z_e^2$ , where  $z_i$  is the activity of an internal monomer and  $z_e$  the activity of a monomer at an endpoint of a rod. No two rods may overlap. The limit  $z_i = 0$  maps onto the dimer model, while the limit  $z_e \rightarrow 0$  corresponds to rods of infinite length. In general, the mean length of rods and the density of occupied lattice sites will be determined by the activities  $z_i$  and  $z_e$ . We obtain the thermodynamic behavior of the system by finding the solution on strips of width  $L$  using a transfer matrix method and then applying finite size scaling to extrapolate the results to the limit of infinite width. We show that the system undergoes a continuous isotropic–nematic phase transition as the density of occupied sites is increased, provided the mean number of monomers per rod is high enough. Estimates of the critical exponents are consistent with the transition being in the the Ising universality class. No high density transition from the nematic phase to an isotropic phase is found within this model.

An exact solution exists for a particular case of the model, when it may be mapped onto the two dimensional Ising model [47]. In this solvable case, the activity of a rod with  $k$  monomers is  $2^{-k} q^{1-k}$ . This corresponds to the choice  $z_e = \sqrt{z_i/2}$ . A continuous Ising transition between an isotropic and a nematic phase occurs at a critical value  $q_c = 1/(2 + 2\sqrt{2})$ , corresponding to  $z_i = 1 + \sqrt{2}$ ,  $z_e = \sqrt{(1 + \sqrt{2})/2}$  being a point on the critical line [47]. Our transfer matrix results for this value of  $z_i$  and  $z_e$  are consistent with the exact solution.

The rest of the paper is organized as follows. In Sec. II

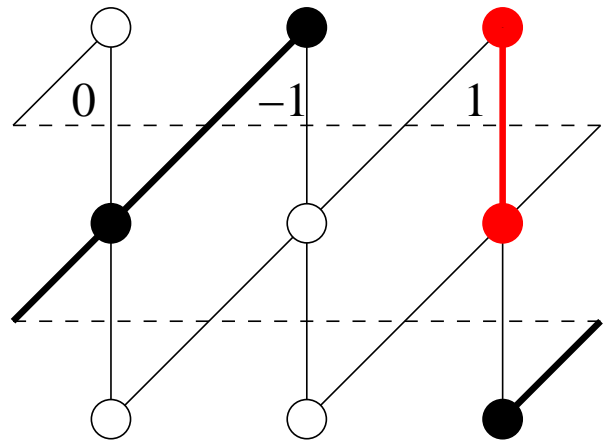


FIG. 1. A strip of width  $L = 3$  with periodic boundary condition in the horizontal direction. The successive states are defined by the configurations of the edges crossing the dashed lines. Part of a rod in the  $x$  direction (black) and of another in the  $y$  direction (red) are shown. The indices 0, -1, 1 define the state of the upper set of  $L$  pairs of  $x$  and  $y$  edges. The transfer is in the vertical direction.

we define the transfer matrix for the model on strips. In Sec. III the critical behavior of the model is obtained. The results for fully packed limit is contained in Sec. III A and those for finite density in Sec. III B. Section IV contains a discussion of results and some open problems.

## II. TRANSFER MATRIX SOLUTION ON STRIPS

We study the model on strips of finite width  $L$ , and extrapolate our results to the two-dimensional thermodynamic limit  $L \rightarrow \infty$ . We define the width of the strip as equal to the number of sites aligned horizontally across the strip. In order to treat both directions of the square lattice symmetrically, we rotate the lattice by  $\pi/4$ , so that after a convenient deformation the strip is as shown in Fig. 1. The edges of the square lattice in the  $y$ -direction correspond to vertical edges in Fig. 1, while the edges in  $x$ -direction are at an angle  $\pi/4$  with the horizontal in Fig. 1. Periodic boundary conditions are applied in the horizontal and vertical directions. We note that, with respect to the original lattice, the transfer is in the diagonal direction.

The states used to build the transfer matrix are given by the possible configurations of the edges crossing a horizontal line between sets of horizontal sites, such as the two dashed lines depicted in Fig. 1. They are defined by the occupancy of the edges by bonds belonging to rods. We associate an integer number to each pair of  $x$  and  $y$  edges crossing the dashed line which meet at a lattice site above. Either both edges are empty (index 0), the  $x$  edge is occupied (index -1), or the  $y$  edge is occupied (index 1). For example, in the upper dashed line, no bond belonging to a rod is present in the first pair of lattice edges, from

left to right. Thus, we associate the index 0 to this pair. In the second pair of edges an  $x$ -mer crosses the line, so that a index -1 is associated to this pair. Finally, a  $y$ -mer crosses the third pair, so that a index 1 is associated to it. Therefore, we denote the state of the upper dashed line as  $(0, -1, 1)$ . Similarly, the state of the lower dashed line is  $(-1, 0, 0)$ . We note that all combinations of indices do not represent allowed states, for example, an index 1 may not be followed by an index -1. When  $L = 3$ , there are 18 different states.

The transfer matrix corresponds to the operation of adding a new row of  $L$  sites to the lattice. The configuration of the row of sites between two successive states, as the ones defined by the dashed lines in Fig. 1, determine the matrix element. In the example of Fig. 1, there is one internal monomer and one endpoint monomer, so that the matrix element associated to this pair of states is equal to  $z_i z_e$ . In general, the transfer matrix for this model is not symmetric.

Knowing the transfer matrix, the thermodynamic quantities may be determined. The grand-canonical free energy per site (divided by  $k_B T$ ) of the model in the thermodynamic limit is given by

$$\phi_L(z_i, z_e) = \lim_{L \rightarrow \infty} -\frac{1}{L} \ln \lambda_1(z_i, z_e), \quad (1)$$

where  $\lambda_1$  is the largest eigenvalue of the transfer matrix. The correlation length is given by:

$$\xi_L(z_i, z_e) = \frac{1}{\ln \left( \frac{\lambda_1}{|\lambda_2|} \right)}, \quad (2)$$

where  $\lambda_2$  is the eigenvalue with second largest modulus. In order to look for phase transitions in the two-dimensional limit  $L \rightarrow \infty$ , we use the phenomenological renormalization group argument and, for a given value of  $z_e$ , search for a value of  $z_i$  where the fixed point relation

$$\frac{\xi_L}{L} = \frac{\xi_{L+1}}{L+1}, \quad (3)$$

holds with  $\xi$  as in Eq. (2).

From the largest eigenvalue, other relevant quantities may be calculated as follows. The densities of internal and endpoint monomers in a strip of width  $L$  may be calculated by differentiating the leading eigenvalue with respect to the activities:

$$\rho_{i,L} = \frac{z_i}{L\lambda_{1,L}} \frac{\partial \lambda_{1,L}}{\partial z_i}, \quad (4)$$

$$\rho_{e,L} = \frac{z_e}{L\lambda_{1,L}} \frac{\partial \lambda_{1,L}}{\partial z_e}. \quad (5)$$

The mean number of monomers per rod is given by:

$$\langle k \rangle = \frac{2\rho}{\rho_e}, \quad (6)$$

where  $\rho = \rho_i + \rho_e$  is the fraction of lattice sites occupied by monomers.

The limit of full packing is reached when both activities diverge. More precisely, we consider the limit  $z_e, z_i \rightarrow \infty$  with a fixed ratio

$$r = \frac{z_e}{z_i}, \quad z_e, z_i \rightarrow \infty. \quad (7)$$

This limit may be studied using transfer matrices by taking into account only contributions where all sites are occupied by monomers. From the largest eigenvalue, the fraction of endpoint monomers in the fully packed limit may be found using

$$\rho_{e,L} = \frac{r}{L\lambda_{1,L}} \frac{\partial \lambda_{1,L}}{\partial r}, \quad \rho = 1. \quad (8)$$

The mean number of monomers per rod in this limit is:

$$\langle k \rangle = \frac{2}{\rho_e}, \quad \rho = 1. \quad (9)$$

In the limit of rods of infinite length ( $z_e \rightarrow 0$ ), all eigenvalues may be found easily. It is straightforward to see that the only non-vanishing entries of the transfer matrix are between states where all rods are in the same direction. The total number of states is then  $2^{L+1} - 1$ .

In the spectrum of this transfer matrix, there is one unitary eigenvalue and

$$2 \frac{L!}{m!(L-m)!}$$

eigenvalues of modulus  $z_i^m$ , with  $m = 1, 2, \dots, L$ . The remaining eigenvalues equal zero. Therefore, in this limit, a discontinuous phase transition occurs at  $z_i = 1$  between the empty lattice and a saturated nematic phase where the whole lattice is filled with  $L$  rods in one of the two directions. When  $z_e > 0$ , we do not find any value of  $z_i$  for which the leading eigenvalue is degenerate, although there are vanishing elements in the transfer matrix and thus the hypothesis of the Perron-Frobenius theorem is not fulfilled.

The elements of the transfer matrix are monomials in the activities  $z_e$  and  $z_i$ , and are determined exactly for given widths  $L$  using a computer code. In Table I we show the numbers of states and the numbers of lines of the file with integers defining the transfer matrix, for  $L = 3, 4, \dots, 9$  in the general case and for  $L = 3, 4, \dots, 12$  if only fully packed configurations are allowed. The fraction of non-vanishing elements of the matrix in the general and full lattice cases are also shown in Table I, and it is clear that the matrices are quite sparse. This favors the use of algorithms related to the power method to find the leading eigenvalues of the transfer matrix.

In order to determine numerically the two leading eigenvalues of the transfer matrix, we use a modified version of the algorithm due to Gubenatis and Booth [48]. A brief description of the algorithm is presented in the Appendix. As in all procedures based on the power method,

TABLE I. The numbers of states ( $N_s$ ) and numbers of lines ( $N_l$ ) in the files defining the transfer matrices for the values of the widths ( $L$ ) we considered in the phenomenological renormalization group calculations.  $N_l - N_s$  is the number of non-zero entries in the transfer matrix. The fraction  $f$  of non-zero elements of the matrix is also given. In the last two columns, we indicate the number of lines of the transfer matrix and the fraction of non-vanishing elements restricted to full lattice configurations.

$L$	$N_s$	$N_l$	$f$	$N_{l,fl}$	$f_{fl}$
3	18	217	0.6142	114	0.2963
4	47	1202	0.5229	481	0.1965
5	123	6850	0.4446	2099	0.1306
6	322	39525	0.3781	9332	0.08690
7	843	229330	0.3215	41939	0.05783
8	2207	1333922	0.2734	189665	0.03849
9	5778	7767577	0.2325	860874	0.02561
10	15127	45254202	0.1977	3915689	0.01705
11	39603	-	-	17832219	0.01124
12	103682	-	-	81265636	0.007550

the convergence rate is determined by the spacing between the leading eigenvalues, so that the rates are very low close to the discontinuous transition at  $z_c \rightarrow 0$ .

### III. CRITICAL BEHAVIOR, EXTRAPOLATION OF CRITICAL LINE, AND DENSITIES

In this section, we determine the critical values of the parameters and the exponents describing the transition from transfer matrix calculations on finite strips. The results for the fully packed limit are in Sec. III A and those for other densities in Sec. III B.

#### A. Full Packing

We first estimate the critical value for the ratio of the activities  $r_c$  [see Eq. (7)] in the fully packed limit. Figure 2 shows estimates of  $r_c$  as a function of  $(L + 0.5)^{-1}$ , using pairs of widths  $L$  and  $L + 1$ , corresponding to strips of widths  $L = 3, 4, \dots, 12$ . A non-monotonic behavior is observed at small widths. Therefore, we discard the results obtained from the pairs  $L = 3, 4$  and  $L = 4, 5$ , restricting ourselves to the concave portion of the curve in Fig. 2.

The data for  $r_c(L)$  is fitted to the form  $r_c(L) = r_c + aL^{x_1}$  using three successive values of  $L$ . The estimates of the parameters  $r_c$ ,  $a$  and  $x_1$  from the three pairs  $L, L + 1$ ,  $L + 1, L + 2$ , and  $L + 2, L + 3$  are associated to the width  $L + 3/2$ . The results for the exponent  $x_1$  are shown in Fig. 3. It is apparent that the data are still far from the asymptotic value. However, the value  $x_1 = -3$  is not ruled out by them, and considering the

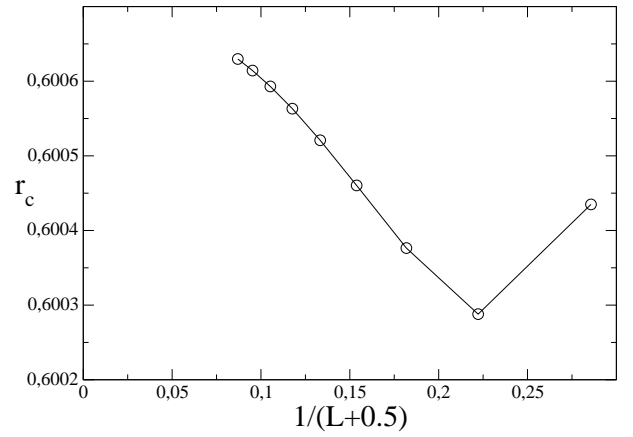


FIG. 2. Estimates for the critical value of the ratio of activities  $r$  in the full lattice limit.

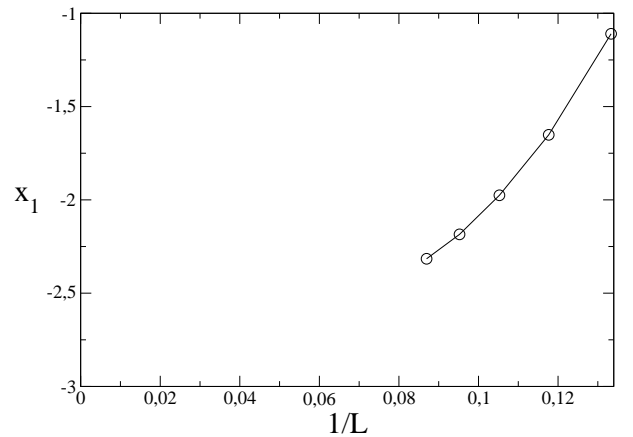


FIG. 3. Estimate of the exponent  $x_1$ , where the critical ratio  $r_c(L)$  is fitted to the form  $r_c(L) = r_c + aL^{x_1}$ . The data are for the fully packed limit.

evidence presented later for the phase transition being in the Ising universality class, we assume  $x_1 = -3$  [49].

We then may obtain two point estimates by fitting the data to the function  $r_c(L) = r_c + aL^{-3}$ . The results for the amplitude  $a$ , presented in Fig. 4, show a clear linear behavior with  $L^{-1}$ . We extrapolate the estimates to  $L \rightarrow \infty$  to obtain  $a = -0.1229$ . Using this value for the amplitude in the behavior of the estimates for the critical ratio as a function of the width, we obtain an extrapolated value  $r_c = 0.6007$ . We note that a unique solution is found for the fixed point of the recursion relation Eq. (3), so that there are no evidences for a second transition at high  $r$ .

We now estimate the mean number of monomers per rod  $\langle k \rangle$  using Eq. (9) at the estimated value of the critical ratio  $r_c$ . In Fig. 5, its variation with  $L^{-1}$  is shown. The extrapolation to the two-dimensional limit, using three point fits to the data, gives  $\langle k \rangle = 4.3978$  at  $r = r_c$ .

The dimensionless free energy per site  $\phi$  of the system in a strip of width  $L$  is given by Eq. (1). Conformal

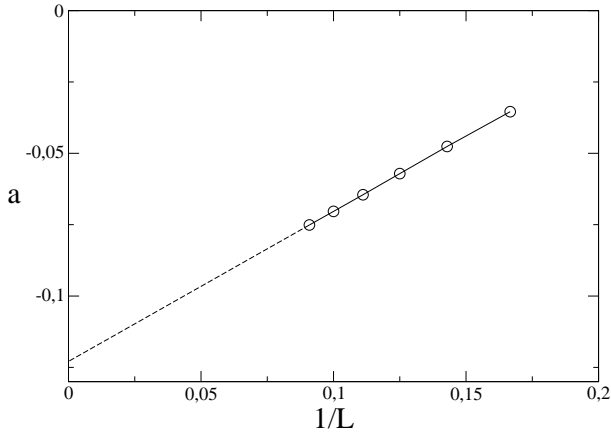


FIG. 4. Estimate of the amplitude  $a$ , where the critical ratio  $r_c(L)$  is fitted to the form  $r_c(L) = r_c + aL^{-1}$ . The data are for the fully packed limit. The dashed line corresponds to the linear extrapolation.

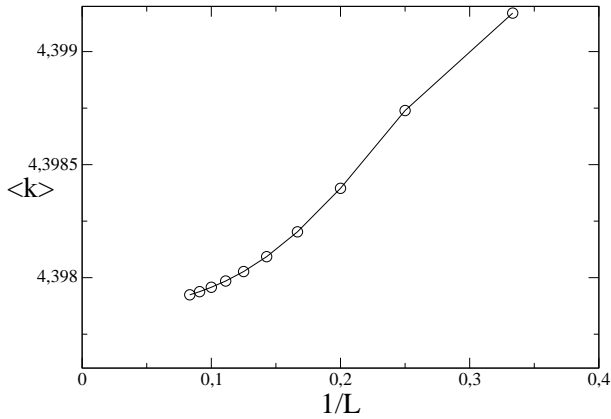


FIG. 5. Estimates for the critical value of the mean number of monomers per rod  $\langle k \rangle$  in the limit of full packing. Results are for widths ranging from  $L = 3$  to  $L = 12$ .

invariance theory states that at the critical condition, for periodic boundary conditions, the free energy obeys [50]:

$$\phi(L) \approx f - \frac{\pi c}{6\ell^2}. \quad (10)$$

where  $c$  is the central charge,  $f$  is the free energy per site in the two-dimensional limit  $\ell \rightarrow \infty$ , and  $\ell$  is the width of the strip measured in units of the lattice parameter. In the usual orientation of the square lattice,  $\ell = L$ , but in the present case, with the lattice rotated by an angle  $\pi/4$ , the width of a strip with  $L$  rows of  $L$  sites is  $\ell = \sqrt{2}L$ , so that we may rewrite the Eq. (10) as

$$\phi(L) \approx f - \frac{\pi c}{12L^2}. \quad (11)$$

Estimates for the central charge may then be obtained by considering free energies at the extrapolated critical ratio for different widths. From the critical free energies

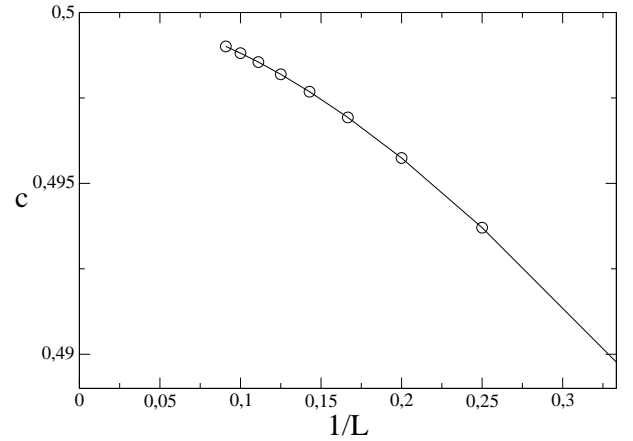


FIG. 6. Estimates of the central charge  $c$  of the model in the limit of full packing obtained from the free energies per site at the estimated critical ratio  $r_c$ .

for two widths, an estimate for  $c$  may be found through:

$$c(L + 1/2) = \frac{12}{\pi} \frac{\phi(L + 1) - \phi(L)}{1/(L + 1)^2 - 1/L^2} \quad (12)$$

The result is shown in Fig. 6, and the convergence of the data to the  $c = 1/2$ , which corresponds to the Ising universality class, is apparent.

Another universal quantity which is rather simple to estimate is the amplitude of the finite size behavior of the inverse correlation length at criticality [51, 52]. The asymptotic behavior of the inverse correlation length is

$$\frac{1}{\xi_\ell} \sim \frac{A}{\ell}, \quad (13)$$

where the correlation length may be calculated using Eq. (2). The amplitude  $A$  is related to the critical exponent  $\eta$ :

$$A = \pi\eta. \quad (14)$$

However, in this result it is implicit that both the correlation length and the width of the strip are measured in units of the lattice spacing. Since each time we apply the transfer matrix we increase the length of the strip by  $\sqrt{2}/2$  lattice spacings, we have  $\xi_\ell = \frac{\sqrt{2}}{2}\xi_L$  and, as discussed above  $\ell = \sqrt{2}L$ , so that we may rewrite Eq. (13) as:

$$\frac{1}{\xi_L} \sim \frac{A}{2L}. \quad (15)$$

The estimate for the critical exponent  $\eta$  are shown in Fig. 7, as a function of  $L^{-1}$ . They are compatible with the value for the Ising universality class  $\eta = 1/4$ .

Finally, we may also estimate the critical exponent  $\nu$  which characterizes the divergence of the correlation length. This may be done by expanding the recursion



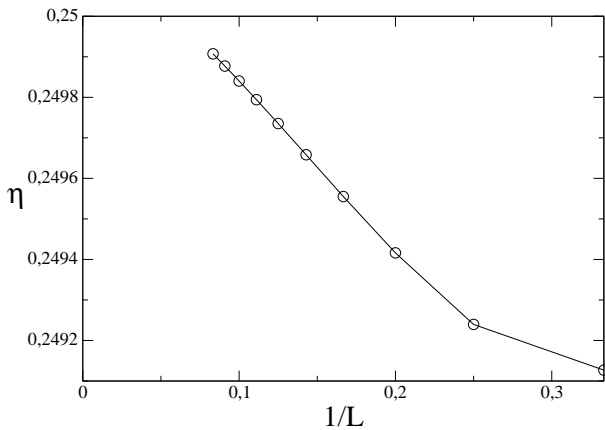


FIG. 7. Estimates of the critical exponent  $\eta$  at full packing, obtained from the amplitudes of the finite size behavior of the correlation length at the estimated critical ratio  $r_c$ .

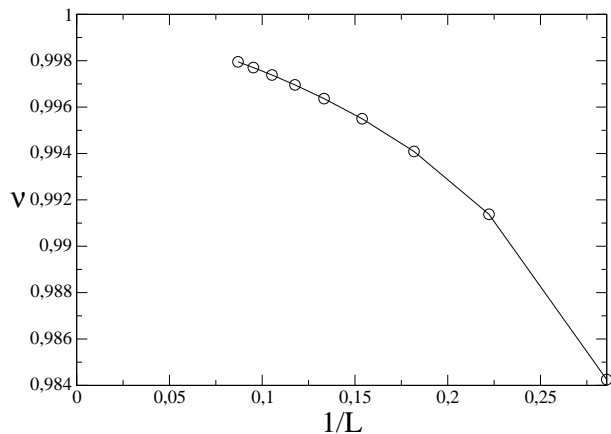


FIG. 8. Estimates of the critical exponent  $\nu$  at full packing, obtained from Eq. (16), at the estimated critical ratio  $r_c$ .

relation of the phenomenological renormalization group close to the fixed point Eq. (3):

$$\nu_L \approx \frac{\ln(\dot{\xi}_L/\dot{\xi}_{L-1})}{\ln[L/(L-1)]} - 1, \quad (16)$$

where the dot stands for a derivative with respect to  $r$ . The results of these calculations are shown in Fig. 8, and again they are consistent with the Ising value  $\nu = 1$ .

From the measured values of the exponents  $\nu$ ,  $\eta$ , and the central charge  $c$  in the thermodynamic limit, we conclude that the isotropic-nematic transition in the fully packed limit belongs to the Ising universality class.

### B. Finite Fugacities

The procedure used to determine the critical behavior of the fully packed limit in Sec. III A is now applied to the transition at finite values of  $z_e$ . For a fixed value of

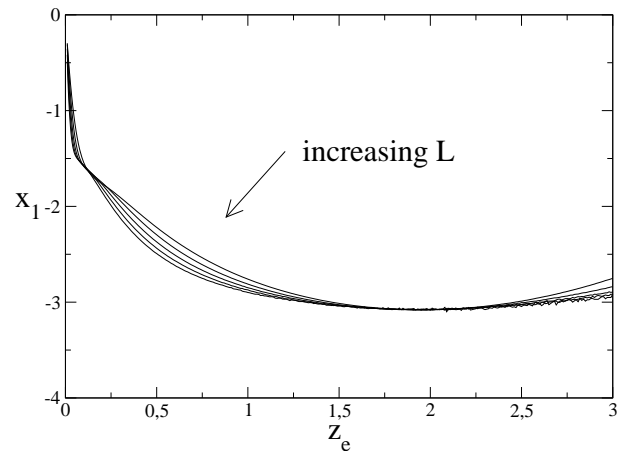


FIG. 9. Estimates of the exponent  $x_1$  characterizing the finite size scaling of the critical activity  $z_{i,c}$  for fixed values of the activity  $z_e$ . In most of the range of values for the activity  $z_e$ , estimates obtained with larger values of  $L$  lead to smaller exponents  $x_1$ , but this is reversed for low values of  $z_e$ .

$z_e$ , we obtain estimates for the critical line [see Eq. (3)] using the correlation lengths for widths  $L$  and  $L + 1$  for  $L$  between 3 and 9. The estimates for the critical values of  $z_i$  for finite width is extrapolated to infinite width by fitting it to the form  $z_{i,c}(L) = z_{i,c} + aL^{x_1}$ . The estimates for the exponent  $x_1$  for a range of  $z_e$  are shown in Fig. 9. As expected, a singular behavior is seen for  $z_e \rightarrow 0$ , since there are no finite size corrections for  $z_e = 0$ . For larger activities estimates are compatible with the Ising value  $x_1 = -3$ , so we adopt this exponent for the whole critical line, with the exception of the singular point  $z_e = 0$ ,  $z_i = 1$ , for which there is no finite size dependence of the estimates and therefore  $x_1 = 0$ .

Once the exponent  $x_1$  is fixed, we perform two point fits to pairs of estimates for  $z_i$ . The phase diagram thus obtained is shown in Fig. 10, where the critical line is the extrapolated result obtained from two point fits to the estimates provided by the largest widths we were able to consider, (8,9) and (9,10). The relative difference between two point fits for the pair of widths (7,8) and (8,9) and the largest widths is less than 0.1% for small values of  $z_e$  and decreases monotonically as  $z_e$  grows, being of the order of  $10^{-4}$  % for  $z_e = 3$ . This may be considered an estimate of the precision of the results for the critical line. The critical line obtained for the exact solution of the model on a four-coordinated Bethe lattice is also shown in Fig. 10. As expected, the Bethe lattice solution overestimates the nematic region. On the dashed line ( $z_e = 2z_i^2$ ), the polydispersed rods model may be mapped on the Ising model [47], as discussed in Sec. I. The corresponding critical point, where this line crosses the critical line, is denoted by a circle.

The phase diagram obtained from both transfer matrices and Bethe lattice show a reentrant behavior at small values of  $z_e$ . In Fig. 11, we zoom in on the phase diagram for small  $z_e$ . Here, the estimates for the critical

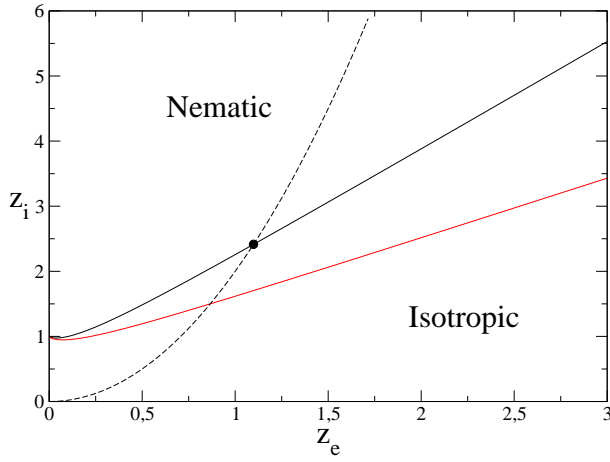


FIG. 10. (color on line) The phase diagram. Extrapolated transfer matrix estimates for the critical line (upper curve, black) and exact results on a four coordinated Bethe lattice (lower curve, red). On the dashed curve the model may be mapped on the Ising model, and the circle corresponds to the critical point of this model.

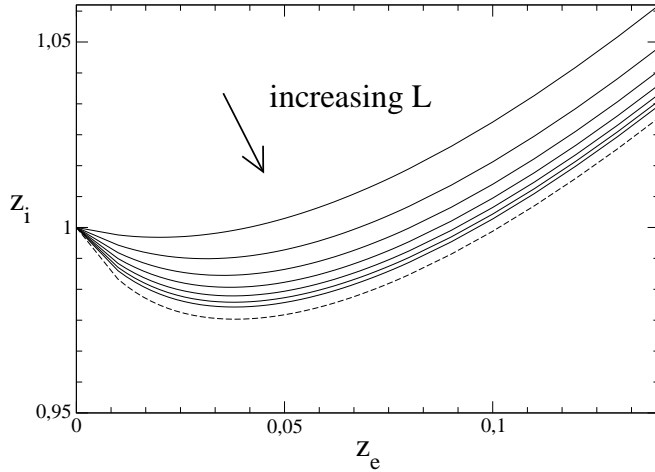


FIG. 11. Details of the region of small values of  $z_e$  of the phase diagram in Fig. 10. The reentrant behavior is visible, as well as the estimates provided by data from distinct pairs of widths. For a given value of  $z_e$ , the estimates for the critical activity  $z_{i,c}$  decrease as the width is increased. The extrapolated critical line is shown by the dashed curve.

values of  $z_i$  for all  $L$  are plotted. The estimates follow a monotonic sequence for increasing widths, showing a clear re-entrance in the thermodynamic limit.

Using the extrapolated data for the critical line in the parameter space of the activities, we may calculate the densities for the model defined on the strips of widths  $L = 3, 4, \dots, 10$ . The results of these calculations are shown in Fig. 12, where the mean number of monomers per rod is plotted as a function of the fraction of lattice sites occupied by monomers. We notice a rather strong finite size dependence of the results at small densities (the estimates for  $\langle k \rangle$  are smaller for larger values of  $\rho$ ).

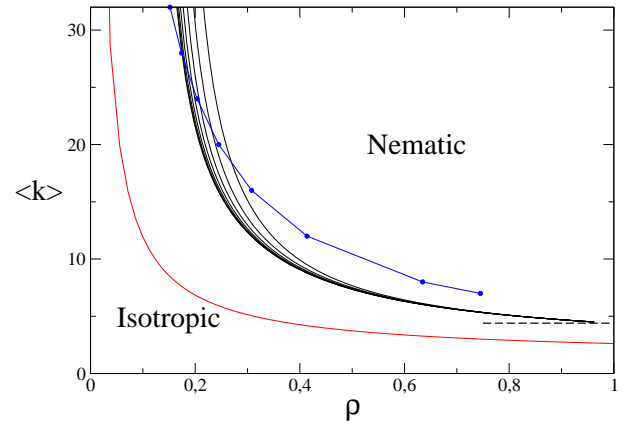


FIG. 12. (color on line) Phase diagram in density variables. The mean number of monomers per rod is shown as a function of the fraction of occupied lattice sites at the transition line. Results for strips of widths  $L = 3, 4, 5, \dots, 10$  are shown (upper curves, black), as well as the Bethe lattice result (lower curve, red). The dashed line corresponds to the estimate of  $\langle k \rangle$  in the full lattice limit. The (blue) dots joined by a line are data from Monte Carlo simulations of the monodispersed case. The data are taken from Ref. [34].

The corresponding result for the Bethe lattice solution is also shown, and again a larger area is occupied by the nematic phase. The full lattice limit for  $\langle k \rangle$ , which was estimated above, is also shown.

We note that, contrary to what was found for monodispersed rods, a single transition from a disordered to a nematic phase is found for polydispersed rods, consistent with the results in the full lattice limit. Thus, in this particular polydispersed model the high density transition is absent. In other words, while the critical  $\langle k \rangle$  for the polydispersed model is a monotonic function of the density  $\rho$ , in the monodispersed case it displays a minimum at a value of  $k$  between 6 and 7. Although the argument supporting a disordered phase in the full packing limit applies for all values of  $k$ , the only case where the high density transition was studied in detail is  $k = 7$  [26].

The critical density at the isotropic–nematic transition for the monodispersed model was recently determined numerically for  $k$  up to 60 [35]. In Fig. 12, these data are compared with the phase boundary of the polydispersed model. For rods with widths between 5 and 6 only the polydispersed model has a nematic phase. We notice that, in general, for a given value of  $\langle k \rangle$  the polydispersed model orders at a smaller density, but apparently this is not the case at sufficiently high values of  $\langle k \rangle$ . However, the results in the low-density region may not be sufficiently precise to confirm this conclusion. In this region of the parameter space the extrapolation procedure we adopted for the critical line may not be trustworthy, since the effective finite size scaling exponent  $x_1$  shown in Fig. 9 changes rapidly with the activity  $z_e$ , due to the proximity of the singular point ( $z_e = 0, z_i = 1$ ). Also, the numerical routines based on the power method become

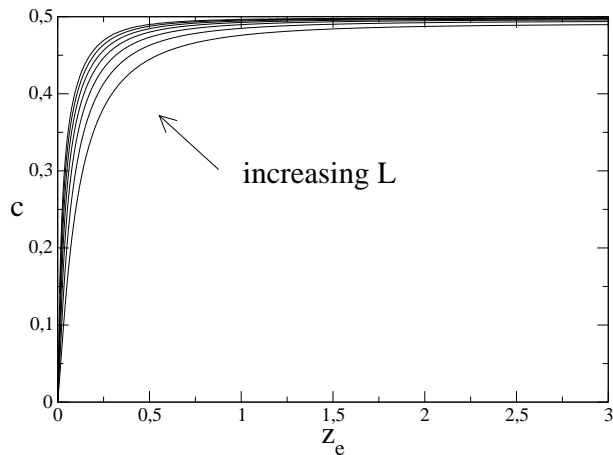


FIG. 13. Estimates for the central charge of the model obtained from the values of the free energy per site at the critical line. Larger estimates are obtained from data for larger widths.

very inefficient as this point is approached, due to the high degeneracy of the leading eigenvalue at this point. Therefore, we are not able to provide compelling evidence of the crossing of critical lines mentioned above.

The estimates for the central charge may now be obtained for the whole critical line. This is accomplished by the same procedure we used in the full lattice limit, through Eq. (12). Results for this estimate as a function of  $z_e$  are plotted in Fig. 13. We found estimates which grow with increasing widths  $L$ . The lowest estimate corresponds to the pair of widths  $L = 3, 4$  and the highest to  $L = 9, 10$ . At the limit  $z_e = 0$  the free energy has no finite size dependence, and therefore  $c = 0$ . The estimates plotted in the graph are consistent with a step function  $c = 0$ , for  $z_e = 0$  and  $c = 1/2$  for  $z_e > 0$ , so that the Ising value found in the full lattice limit extends to finite non-zero values of  $z_e$ .

The critical exponent  $\eta$  may also be estimated at the whole critical line using the amplitude of the correlation length, through Eq. (15). For each of the widths, we generate an estimate for this exponent. The results of these calculations are shown in Fig. 14. The estimates increase with growing widths, so that the smallest value corresponds to  $L = 3$  and the largest to  $L = 10$ . Again the data are consistent with an asymptotic step function behavior, with  $\eta = 0$  for  $z_e = 0$  and the Ising value  $\eta = 1/4$  for  $z_e > 0$ .

Finally, estimates for the exponent  $\nu$  are furnished by the linearization of the phenomenological renormalization group recursion relation at the fixed point [see Eq. (3)]. The results from such calculations, using Eq. (16) for pairs of consecutive widths, are shown in Fig. 15. Again the results are consistent with a convergence to the asymptotic Ising value  $\nu = 1$  for  $z_e > 0$ .

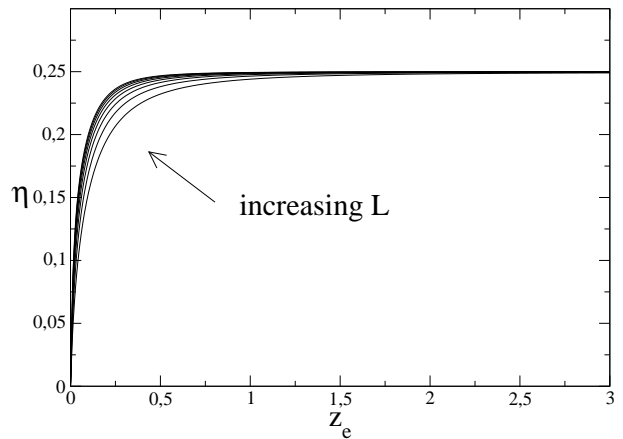


FIG. 14. Estimates for the exponent  $\eta$  obtained from the values of the amplitude of the inverse correlation length at the extrapolated critical line. Larger estimates are obtained from data for larger widths.

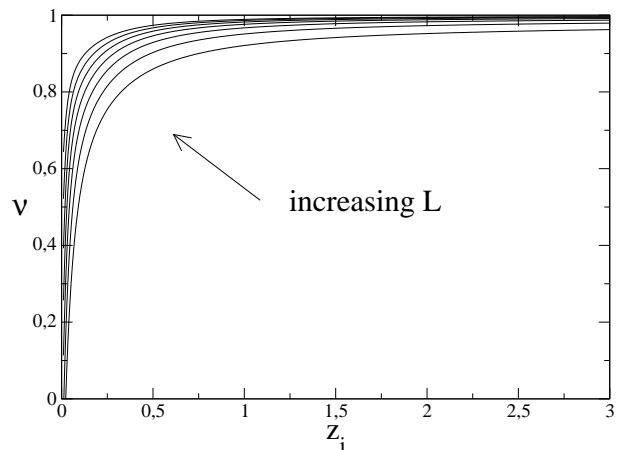


FIG. 15. Estimates for the exponent  $\nu$  model obtained from the linearization of the PRG recursion relation on the critical line. Larger estimates are obtained from data for larger widths.

#### IV. SUMMARY AND DISCUSSION

In this paper, we studied a particular model of poly-dispersed hard rods on a square lattice using transfer matrix techniques. Rods of all sizes are allowed with the weight of a rod of length  $k$  being  $z_i^{k-2} z_e^2$ , where  $z_i$  ( $z_e$ ) is the activity for an internal (endpoint) monomer. We showed that the system undergoes a single isotropic-nematic transition as  $z_i$  is increased for a fixed  $z_e$ . The critical exponents and central charge obtained using finite size scaling are shown to be consistent with that of the two dimensional Ising model.

The model studied in this paper is a variant of the model discussed in Ref. [45], used to describe equilibrium polymerization transitions, observed in liquid sulfur. In this model, there are separate weights for the endpoint monomers ( $z_e$ ) and the internal monomers ( $z_i$ )



of the polymeric chains. It may be mapped on the magnetic  $n$ -vector model in the limit where the number of components of the spin  $n$  vanishes. The square of the endpoint monomer activity  $z_e$  corresponds to the magnetic field  $h$  of the magnetic model. Therefore, the phase transition in this model occurs when  $z_e = 0$ , that is, for infinite polymeric chains. Also, the original model considers flexible chains. Both these conditions are satisfied in the equilibrium polymerization transition in liquid sulfur. In particular, for sulfur at the polymerization temperature,  $z_e \approx 10^{-12}$ . An experimental realization of the model studied in this paper would be a situation where the value of  $z_i$  is finite and the chains are rigid. In this limit, our model predicts an isotropic-nematic phase transition.

Contrary to what was found for monodispersed rods, the nematic phase remains stable up to the limit of full packing. If, in the monodispersed system, a small density of rods of different length are added, then the two transitions present in the monodispersed system should persist. However, in the model considered in this paper, once the density of occupied sites and the mean length of the rods are fixed, the polydispersity is also determined. It would be interesting to consider a situation where the polydispersity could be independently changed, in order to find out what amount of polydispersity is necessary to destroy the high density transition from the nematic to the isotropic phase.

Our estimates for the critical parameters are consistent with those of the two dimensional Ising universality class, which is an expected result if we consider the symmetry of the order parameter. This should change, for example, if the model is defined on the triangular or hexagonal lattices, where we expect the universality class to be the that of the  $q = 3$  Potts model, as was found for the isotropic-nematic transition in the case of monodispersed rods [29, 30].

The transfer matrix technique used in the paper was well suited for the particular choice of statistical weight for a rod. The number of indices required to label a state in the transfer matrix is only 3. This should be compared with the  $2k + 1$  indices required to label a state in the problem of monodispersed rods of length  $k$ . This makes it difficult to study mono-dispersed problems using transfer matrices. However, there are some examples where transfer matrix could be useful. One is the case of polydispersed rectangles of size  $2 \times k$  with the same weight as that studied in this paper. The number of indices to label a state is now 5, making it suitable for transfer matrix calculations. It would be interesting to see which of three transitions present in the monodispersed problem [34–36] persist. Another problem is that of mixtures of hard squares and dimers which was recently shown to have a very interesting phase diagram including a Berezinskii-Kosterlitz-Thouless transition in the fully packed limit [53]. The number of indices now required to label a state is only 5 making it suitable for transfer matrix studies. The fully packed limit is simpler

since the number of states and indices are fewer. The same will be true for mixtures of particles with the first  $k$  nearest neighbors excluded when  $k$  is small [54, 55]. These are promising areas for future study.

## ACKNOWLEDGMENTS

JFS acknowledges Francisco C. Alcaraz and Marcelo S. Sarandy for helpful discussions and CNPq for financial support.

## Appendix: The Gubenatis-Booth (GB) algorithm

In the paper, the leading eigenvalues of the transfer matrix were determined using an algorithm that is a slightly modified version of the algorithm proposed by Gubenatis and Booth [48]. In this appendix, we briefly describe the method. A more detailed discussion may be found in the original paper.

This method is a variant of the power method to find the largest eigenvalue of a real matrix  $\mathbf{A}$ . Its simplest implementation consists of starting with an arbitrary normalized vector  $\psi$  and performing a two step iteration:  $\phi = \mathbf{A}\psi$  and  $\psi = \phi/||\phi||$ , where the normalization procedure is quite arbitrary. It may then be shown that, as long as the starting vector is not orthogonal to the (right) eigenvector  $\psi_1$  associated with the largest eigenvalue  $\lambda_1$  and the eigenvalue is non-degenerate, the iteration converges to  $\psi \rightarrow \psi_1/||\psi_1||$  and  $||\phi|| \rightarrow \lambda_1$ . The error, after  $n$  steps, is proportional to  $(|\lambda_2/\lambda_1|)^n$ , where  $\lambda_2$  is the second largest eigenvalue in absolute value. If the matrix is non-symmetric, both left and right eigenvectors need to be considered.

If the second largest eigenvalue is also required, one possibility is to iterate with two orthogonal vectors, so that one converges to  $\psi_1$  and the other to  $\psi_2$  [56]. Alternatively, the GB algorithm starts from the observation that any non-zero component  $\alpha$  of an eigenvector belonging to the eigenpair  $(\lambda, \psi)$  on the matrix  $\mathbf{A}$  obeys

$$\lambda = \frac{\sum_{\beta} A_{\alpha,\beta} \psi_{\beta}}{\psi_{\alpha}}. \quad (\text{A.1})$$

This identity may be extended to sums of any grouping  $R_i$  of components:

$$\lambda = \frac{\sum_{\alpha \in R_1} \sum_{\beta} A_{\alpha,\beta} \psi_{\beta}}{\sum_{\alpha \in R_1} \psi_{\alpha}} = \frac{\sum_{\alpha \in R_2} \sum_{\beta} A_{\alpha,\beta} \psi_{\beta}}{\sum_{\alpha \in R_2} \psi_{\alpha}} = \dots \quad (\text{A.2})$$

When only the two largest eigenvalues are needed, the iterative procedure starts with two vectors  $\psi' = \sum_i a_i \psi_i$  and  $\psi'' = \sum_i b_i \psi_i$ , and the behavior of the vector  $\psi = (1 - \eta)\psi' + \eta\psi''$  under iteration is considered, where  $\eta$  is a number. Assuming that after  $n$  iterations only the two dominant eigenpairs are significant, we have:

$$\mathbf{A}^n \psi = \sum_{i=1,2} [(1 - \eta)a_i + \eta b_i] \lambda_i^n \psi_i. \quad (\text{A.3})$$

The parameter  $\eta$  is adjusted at each step to prevent the  $\psi$  from collapsing to the dominant eigenvector. This is accomplished by choosing two groupings of components

$R_1$  and  $R_2$  and requiring that the condition Eq. (A.2) is fulfilled at each step. So, for example, after  $n$  iterations the estimates  $\kappa$  of the eigenvalue for each grouping are:

$$\kappa_1 = \frac{[(1-\eta)a_1 + \eta b_1]\lambda_1^n \sum_{\alpha \in R_1} \psi_{1,\alpha} + [(1-\eta)a_2 + \eta b_2]\lambda_2^n \sum_{\alpha \in R_1} \psi_{2,\alpha}}{[(1-\eta)a_1 + \eta b_1]\lambda_1^{n-1} \sum_{\alpha \in R_1} \psi_{1,\alpha} + [(1-\eta)a_2 + \eta b_2]\lambda_2^{n-1} \sum_{\alpha \in R_1} \psi_{2,\alpha}}, \quad (\text{A.4})$$

$$\kappa_2 = \frac{[(1-\eta)a_1 + \eta b_1]\lambda_1^n \sum_{\alpha \in R_2} \psi_{1,\alpha} + [(1-\eta)a_2 + \eta b_2]\lambda_2^n \sum_{\alpha \in R_2} \psi_{2,\alpha}}{[(1-\eta)a_1 + \eta b_1]\lambda_1^{n-1} \sum_{\alpha \in R_2} \psi_{1,\alpha} + [(1-\eta)a_2 + \eta b_2]\lambda_2^{n-1} \sum_{\alpha \in R_2} \psi_{2,\alpha}}, \quad (\text{A.5})$$

Now, at each step of the iteration, one requires  $\kappa_1 = \kappa_2$ , which leads to a quadratic equation for the parameter  $\eta$ . One solution  $(1-\eta)a_1 + b_1\eta = 0$  guides the process to the second eigenpair  $\kappa_1 = \kappa_2 = \lambda_2$ , while the other  $(1-\eta)a_2 + b_2\eta = 0$  leads it to the second eigenpair  $\kappa_1 = \kappa_2 = \lambda_1$ .

Now, if the vectors at some step of the iterative process are  $\psi'$  and  $\psi''$ , then we determine  $\hat{\psi}' = \mathbf{A}\psi'$  and  $\hat{\psi}'' = \mathbf{A}\psi''$ . The consistency condition will be:

$$\frac{(1-\eta)s_{11} + \eta s_{12}}{(1-\eta)r_{11} + \eta r_{12}} = \frac{(1-\eta)s_{21} + \eta s_{22}}{(1-\eta)r_{21} + \eta r_{22}}, \quad (\text{A.6})$$

where the sums of components are defined as:

$$s_{i,1} = \sum_{\alpha \in R_i} \hat{\psi}'_{\alpha}, \quad (\text{A.7})$$

$$s_{i,2} = \sum_{\alpha \in R_i} \hat{\psi}''_{\alpha}, \quad (\text{A.8})$$

$$r_{i,1} = \sum_{\alpha \in R_i} \psi'_{\alpha}, \quad (\text{A.9})$$

$$r_{i,2} = \sum_{\alpha \in R_i} \psi''_{\alpha}. \quad (\text{A.10})$$

The consistency condition Eq. (A.6) leads to a quadratic equation for the parameter  $\eta$ :

$$a_2\eta^2 + a_1\eta + a_0 = 0, \quad (\text{A.11})$$

where the coefficients are given in terms of the sums:

$$a_0 = r_{12}s_{11} - r_{11}s_{12}, \quad (\text{A.12})$$

$$a_1 = 2(r_{11}s_{12} - r_{12}s_{11}) + r_{22}s_{11} + r_{12}s_{21} - r_{21}s_{12} - r_{11}s_{22}, \quad (\text{A.13})$$

$$a_2 = r_{12}s_{11} + r_{22}s_{21} + r_{21}s_{12} + r_{11}s_{22} - r_{11}s_{12} - r_{21}s_{22} - r_{22}s_{11} - r_{12}s_{21}. \quad (\text{A.14})$$

Further refinements of the algorithm that results in faster convergence may be found in the original article [48].

We summarize the steps of the algorithm.

1. Define small convergence parameters  $\epsilon_1$  and  $\epsilon_2$ . In our double precision calculations, we have chosen  $\epsilon_1 = \epsilon_2 = 10^{-13}$ .
2. Make initial guesses for vectors  $\psi'$  and  $\psi''$ , and the groupings of components  $R_1$  and  $R_2$ . If the matrix  $\mathbf{A}$  is of size  $N \times N$ , we have chosen  $R_1 = (1, 2, \dots, [N/2])$  and  $R_2 = [N/2] + 1, [N/2] + 2, \dots, N$ .
3. Normalize:  $\psi' \leftarrow \psi' / \|\psi'\|$ ,  $\psi'' \leftarrow \psi'' / \|\psi''\|$ .
4. Obtain  $\hat{\psi}' = \mathbf{A}\psi'$  and  $\hat{\psi}'' = \mathbf{A}\psi''$ .
5. Find the two values of  $\eta$  for which consistency condition [see Eq. (A.11)] is satisfied. If the roots are complex, update vectors ( $\psi' \leftarrow \hat{\psi}'$  and  $\psi'' \leftarrow \hat{\psi}''$ ) and return to step 3.
6. Find estimates of eigenvalues associated to the two real values of  $\eta$ , using, for example, the grouping  $R_1$ :

$$\lambda = \frac{(1-\eta)s_{11} + \eta s_{21}}{(1-\eta)r_{11} + \eta r_{21}}. \quad (\text{A.15})$$

Define  $\eta_1$  to be the solution associated to the largest eigenvalue  $\lambda_1$  and  $\eta_2$  related to the second largest eigenvalue  $\lambda_2$ .

7. Check for convergence: If  $|\eta_1| > \epsilon_1$  or  $|1 - \eta_2| > \epsilon_2$  update vectors  $\psi' \leftarrow (1 - \eta_1)\hat{\psi}' + \eta_1\hat{\psi}''$ ,  $\psi'' \leftarrow (1 - \eta_2)\hat{\psi}' + \eta_2\hat{\psi}''$  and return to step 3.
8. Terminate.

[1] P. G. de Gennes and J. Prost, *The Physics of Liquid Crystals* (Oxford University Press, Oxford, 1995) pp. 64–66.

[2] S. Fraden, G. Maret, D. L. D. Caspar, and R. B. Meyer, Phys. Rev. Lett. **63**, 2068 (1989).

[3] M. F. Islam, A. M. Alsayed, Z. Dogic, J. Zhang, T. C.

- Lubensky, and A. G. Yodh, Phys. Rev. Lett. **92**, 088303 (2004).
- [4] L. Onsager, Ann. N.Y. Acad. Sci. **51**, 627 (1949).
- [5] P. J. Flory, Proc. R. Soc. **234**, 60 (1956).
- [6] R. Zwanzig, J. Chem. Phys. **39**, 1714 (1963).
- [7] G. J. Vroege and H. N. W. Lekkerkerker, Rep. Prog. Phys. **55**, 1241 (1992).
- [8] N. D. Mermin and H. Wagner, Phys. Rev. Lett. **17**, 1133 (1966).
- [9] V. L. Berezinskii, Sov. Phys. JETP **32**, 493 (1971).
- [10] V. L. Berezinskii, Sov. Phys. JETP **34**, 610 (1972).
- [11] J. M. Kosterlitz and D. J. Thouless, J. Phys. C: Solid State Phys. **6**, 1181 (1973).
- [12] J. P. Straley, Phys. Rev. A **4**, 675 (1971).
- [13] D. Frenkel and R. Eppenga, Phys. Rev. A **31**, 1776 (1985).
- [14] M. D. Khandkar and M. Barma, Phys. Rev. E **72**, 051717 (2005).
- [15] R. L. C. Vink, Euro. Phys. J. B **72**, 225 (2009).
- [16] O. J. Heilmann and E. H. Lieb, Phys. Rev. Lett. **24**, 1412 (1970).
- [17] H. Kunz, Phys. Lett. A **32**, 311 (1970).
- [18] C. Gruber and H. Kunz, Commun. Math. Phys. **22**, 133 (1971).
- [19] O. J. Heilmann and E. Lieb, Commun. Math. Phys. **25**, 190 (1972).
- [20] R. Dickman, J. Chem. Phys. **136**, 174105 (2012).
- [21] F. Alet, J. L. Jacobsen, G. Misguich, V. Pasquier, F. Mila, and M. Troyer, Phys. Rev. Lett. **94**, 235702 (2005).
- [22] S. Papanikolaou, D. Charrier, and E. Fradkin, Phys. Rev. B **89**, 035128 (2014).
- [23] A. Ghosh and D. Dhar, Euro. Phys. Lett. **78**, 20003 (2007).
- [24] M. Disertori and A. Giuliani, Commun. Math. Phys. **323**, 143 (2013).
- [25] J. Kundu, R. Rajesh, D. Dhar, and J. F. Stilck, AIP Conf. Proc. **1447**, 113 (2012).
- [26] J. Kundu, R. Rajesh, D. Dhar, and J. F. Stilck, Phys. Rev. E **87**, 032103 (2013).
- [27] D. Dhar, R. Rajesh, and J. F. Stilck, Phys. Rev. E **84**, 011140 (2011).
- [28] J. Kundu and R. Rajesh, Phys. Rev. E **88**, 012134 (2013).
- [29] D. A. Matoz-Fernandez, D. H. Linares, and A. J. Ramirez-Pastor, Euro. Phys. Lett. **82**, 50007 (2008).
- [30] D. A. Matoz-Fernandez, D. H. Linares, and A. J. Ramirez-Pastor, Physica A **387**, 6513 (2008).
- [31] D. A. Matoz-Fernandez, D. H. Linares, and A. J. Ramirez-Pastor, J. Chem. Phys. **128**, 214902 (2008).
- [32] D. H. Linares, F. Romá, and A. J. Ramirez-Pastor, J. Stat. Mech., P03013 (2008).
- [33] T. Fischer and R. L. C. Vink, Euro. Phys. Lett. **85**, 56003 (2009).
- [34] J. Kundu and R. Rajesh, Phys. Rev. E **89**, 052124 (2014).
- [35] J. Kundu and R. Rajesh, arXiv preprint arXiv:1409.4569 (2014).
- [36] T. Nath, J. Kundu, and R. Rajesh, arXiv preprint arXiv:1411.7831 (2014).
- [37] P. A. Buining and H. N. W. Lekkerkerker, J. Phys. Chem. **97**, 11510 (1993).
- [38] M. P. B. van Bruggen, F. M. van der Kooij, and H. N. W. Lekkerkerker, J. Phys.: Condensed Matter **8**, 9451 (1996).
- [39] H. N. W. Lekkerkerker, P. Coulon, R. Van Der Haegen, and R. Deblieck, J. Chem. Phys. **80**, 3427 (1984).
- [40] T. Birshtein, B. Kolegov, and V. Pryamitsyn, Poly. Sci. U.S.S.R. **30**, 316 (1988).
- [41] A. Speranza and P. Sollich, J. Chem. Phys. **118**, 5213 (2003).
- [42] A. Speranza and P. Sollich, Phys. Rev. E **67**, 061702 (2003).
- [43] N. Clarke, J. A. Cuesta, R. Sear, P. Sollich, and A. Speranza, J. Chem. Phys. **113**, 5817 (2000).
- [44] Y. Martínez-Ratón and J. A. Cuesta, J. Chem. Phys. **118**, 10164 (2003).
- [45] J. C. Wheeler, S. J. Kennedy, and P. Pfeuty, Phys. Rev. Lett. **45**, 1748 (1980).
- [46] J. C. Wheeler and P. Pfeuty, Phys. Rev. A **24**, 1050 (1981).
- [47] D. Ioffe, Y. Velenik, and M. Zahradnik, J. Stat. Phys. **122**, 761 (2006).
- [48] J. Gubernatis and T. Booth, J. Comp. Phys. **227**, 8508 (2008).
- [49] W. Guo and H. W. J. Blöte, Phys. Rev. E **66**, 046140 (2002).
- [50] H. W. J. Blöte, J. L. Cardy, and M. P. Nightingale, Phys. Rev. Lett. **56**, 742 (1986).
- [51] M. P. Nightingale and H. W. J. Blöte, J. Phys. A **16**, L657 (1983).
- [52] J. L. Cardy, J. Phys. A **17**, L385 (1984).
- [53] K. Ramola, K. Damle, and D. Dhar, arXiv preprint arXiv:1408.4943 (2014).
- [54] H. C. M. Fernandes, J. J. Arenzon, and Y. Levin, J. Chem. Phys. **126**, 114508 (2007).
- [55] T. Nath and R. Rajesh, Phys. Rev. E **90**, 012120 (2014).
- [56] J. H. Wilkinson, *The Algebraic Eigenvalue Problem* (Oxford University Press, Oxford, 1965).